Solvent Effects on the Photodissociation of Formic Acid: A Theoretical Study

Yan-Cong Tian and Wei-Hai Fang*

Department of Chemistry, Beijing Normal University, Beijing 100875, P. R. China

Received: June 25, 2006; In Final Form: August 18, 2006

Photodissociation of aqueous formic acid has been investigated with the CASSCF, DFT, and MR-CI methods. Solvent effects are considered as a combination of the hydrogen-bonding interaction from explicit H_2O molecules and the effects from the bulk surrounding H_2O molecules using the polarizable continuum model. It is found that the hydrogen-bonding effect from the explicit water in the complex is the major factor to influence properties of aqueous formic acid, while the bulk surrounding H_2O molecules has a noticeable influence on the structures of the complex. The direct C−O bond fission along the S_1 pathway is predicted to be an important channel upon photolysis of aqueous formic acid at 200 nm, which is consistent with experimental observation that aqueous formic acid dissociates predominantly into fragments of HCO and OH. The existence of a dark channel upon photolysis of aqueous formic acid at 200 nm is assigned as fast relaxation from the S_1 Franck−Condon geometry to the T_1/S_1 intersection and subsequent $S_1 \rightarrow T_1$ intersystem crossing process. $S_1 \rightarrow S_0$ internal conversion followed by molecular elimination to CO + H_2O is the most probable primary process for formation of carbon monoxide, which was observed with considerable yield upon photolysis of aqueous formic acid at 253.7 nm.

Introduction

Formic acid (HCOOH) is an important intermediate in the oxidation of unsaturated hydrocarbons in combustion.[1] Of the organic molecules observed in the interstellar medium and upper troposphere of the earth, particular attention has been devoted to formic acid[2] since it plays an important role in the chemistry of interstellar space and is among the most abundant pollutants in the atmosphere.[3,4] HCOOH is a molecule of great interest to experimental and theoretical chemists because it is the simplest of the organic acids and presents itself as an ideal model compound for spectroscopic and theoretical studies of the carboxylic acids and related organic compounds.

Photodissociation of formic acid in the gas phase has been studied extensively.[5−20] The three dissociation channels that can occur in the HCOOH photolysis are given as follows

$$\mathrm{HCOOH} + h\nu \rightarrow \mathrm{HCO} + \mathrm{OH} \quad (1)$$

$$\rightarrow \mathrm{H} + \mathrm{COOH} \quad (2)$$

$$\rightarrow \mathrm{HCOO} + \mathrm{H} \quad (3)$$

A quantum yield of 0.7−0.8 was determined for formation of the OH product.[9−14] S_1 direct dissociation to HCO + OH was found to be a dominant pathway for HCOOH photolysis at 220−193 nm.[15−20] Meanwhile, a small amount of CO and CO_2 were observed as a result of internal conversion to the ground state.

Several theoretical studies have been done in order to explore the S_0 structures of *cis*- and *trans*-HCOOH,[21−23] the barrier to the isomerization in the ground state,[24−26] and thermal decomposition.[27−30] All of these studies agree that the most important reactions in the ground state are molecular eliminations of HCOOH to CO + H_2O and CO_2 + H_2. The barriers to the two reactions are in the range of 68−71 kcal/mol. As a complementary of experiments, CIS and CASSCF methods were to used to calculate the excited-state potential-energy profiles of HCOOH in the gas phase.[31,18] A combined CASSCF/MR-CI calculation has been performed toward understanding wavelength-dependent photodissociation processes of formic acid in the gas phase.[32] Very recently, adiabatic and nonadiabatic molecular dynamics studies have been performed to simulate photoinduced radical and molecular dissociation processes of gaseous formic acid.[33,34]

As stated above, the photochemistry of gas-phase formic acid has been reported plenty from both experimental and theoretical points of view. In comparison, photolysis of aqueous formic acid drew less attention from chemists. In a solution environment the influences exerted on the solute molecules by solvent and secondary or tertiary reactions of the photoproducts make the photochemistry of aqueous formic acid more complicated. Early in 1962 carbon monoxide was observed with considerable yield upon photolysis of aqueous formic acid at 253.7 and 184.9 nm.[35] Two separation pathways, HCOOH → HCO → CO and HCOOH → COOH → CO, were suggested to be responsible for formation of CO. In oxygen-free solutions, only the 184.9 nm wavelength can give rise to removal of formic acid. Photolysis of aqueous formic acid was found to lead to production of carbon monoxide, carbon dioxide, oxalic acid, and the oxalic acid formyl ester.[36] Femtosecond transient absorption spectroscopy was used to investigate the primary reaction dynamics of aqueous formic acid following photoexcitation of the $n \rightarrow \pi^*$ transition at 200 nm.[37] It was found that aqueous formic acid dissociates predominantly into fragments of HCO and OH. Meanwhile, the measured transient absorption shows that a dark channel exists with a time constant of ∼170 ps. Unfortunately, the very low extinction coefficient of formic acid precludes a detailed experimental investigation of the nature of the dark channel. In addition, photoinduced decomposition of HCOOH has been investigated in low-temperature matrixes, and conformational memory was observed in photoinduced dissociation processes of formic acid at 193 nm.[31,38,39]

* To whom correspondence should be addressed. Phone: (+86)-10−5880−5382. E-mail: fangwh@bnu.edu.cn.

10.1021/jp063967j CCC: $33.50
Published on Web 09/26/2006

Unlike the photochemistry of formic acid in the gas phase, the photodissociation mechanism of aqueous formic acid remains largely unknown. To our knowledge, photodissociation dynamics has not been theoretically studied for formic acid in the solution phase. In an attempt to understand the underlying mechanism of HCOOH photolysis in an aqueous environment, we present a theoretical study on the mechanistic photodissociation of aqueous formic acid with advanced electronic structure methods in this work. Effects of the solvent are considered from two aspects. On one hand, a hydrogen-bond complex is formed between formic acid and water. On the other hand, the interaction between the complex and solvent is taken into account with a polarizable continuum model (PCM). We believe that the results reported here provide new insights into the photodissociation dynamics of formic acid and the related compounds in the aqueous environment.

Computational Details

The band origin of the $\pi \rightarrow \pi^*$ transition was experimentally assigned at 8.1 eV (~150 nm) for formic acid in the gas phase. Therefore, photoexcitation in the UV region (248−185 nm) initially leads to HCOOH molecules in the $^1n\pi^*(S_1)$ state. Electronic states considered here in addition to the ground state are the excited valence singlet and triplet states, $^1n\pi^*(S_1)$ and $^3n\pi^*(T_1)$, which are related to photodissociation processes of formic acid. Since the $^1n\pi^*$ and $^3n\pi^*$ states are quite different from the S_0 state in geometry, we performed principal calculations at the complete active space self-consistent field (CASSCF) level of theory, which has been proved to be efficient in modeling great changes in electronic structure of a molecule system.[40] Three different active spaces were used in the study of photodissociation dynamics of formic acid in the gas phase,[32] which are composed of 18 electrons (all valence electrons for HCOOH) in 13 orbitals (18,13), 10 electrons in 8 orbitals (10,8), and 8 electrons in 7 orbitals (8,7). It was found that the CAS(10,8)-optimized structural parameters and calculated relative energies for HCOOH in the S_0, S_1, and T_1 states are very close to those from the CAS(18,13) calculations. In this work, we employed the active space of 10 electrons in 8 orbitals, originating from the C═O π and π^* orbitals, C−O and C−H σ and σ^* orbitals, the two oxygen nonbonding orbitals. All calculations were performed with the cc-pVTZ basis set.[41]

The influence of solvent can be defined as a combination of the hydrogen-bonding interaction from explicit solvent molecules and the effects from the bulk surrounding solvent molecules. Hydrogen-bonding interaction between HCOOH and H_2O could play an important role in photodissociation dynamics of aqueous formic acid. Therefore, structures of the HCOOH−H_2O complexes in the S_0, T_1, and S_1 states were optimized with the CAS(10,8) method. Once convergence was reached, the harmonic frequencies were examined to confirm the optimized structure to be a true minimum or saddle point. For comparison, structures and energies of the complexes in the S_0 and T_1 state are also calculated at the B3LYP level of theory. To evaluate the importance of the bulk solvent effects added to the hydrogen-bond complexes, we employed self-consistent reaction field (SCRF) methods to determine the structures and energies of the complexes in the three lowest electronic states at the CAS(10,8) level. A dielectric constant of 78.93 was used for the water bulk using the polarizable continuum model (PCM)[42] in which the cavity is created via a series of overlapping spheres. The radii of the spheres were obtained from the united atom topological model,[43] and the number of initial tesserae/atomic spheres was set to 60. To confirm the nature of the stationary points and produce theoretical activation parameters, harmonic frequencies were also calculated for all structures optimized with the PCM model. Structural optimizations described here have been performed with the Gaussian 03 package of programs.[44] To refine the relative energies of the stationary structures, the single-point energies for some structures were calculated with the internally contracted MR-CI method that includes all single and double excitations relative to the CAS(10,8) reference wave functions. The MOLPRO program package[45] was used to perform the MR-CI single-point energy calculations.

Results and Discussion

A. Equilibrium Geometries and Their Relative Energies. As is well known, there are two conformers for formic acid in the S_0 state with the acidic hydrogen aligned toward the oxygen atom of the carbonyl group or away from it. Their complexes with water in the S_0 state have been extensively studied in the past decades. There are multiple minima structures for complexes of formic acid with one water molecule aligning in different directions around the formic acid. Among them the most stable conformation is a cyclic complex with both the water and formic acid acting as hydrogen donor and acceptor, resulting in two relatively strong hydrogen bonds.[46,47] The cyclic complex of formic acid with one water has been observed experimentally.[48,49] The calculated intermolecular frequencies for the one-water complex of formic acid are close to those observed experimentally for aqueous formic acid,[49] which provides evidence that the H-bonded complexes in aqueous formic acid exist mainly in the form of the cyclic complex with one water. Here, we considered the cyclic complex of *trans*-HCOOH with one water molecule as the initial reactant for investigating photodissociation processes of aqueous formic acid.

The optimized structures for gaseous and aqueous complexes in the S_0, S_1, and T_1 states are depicted in Figure 1 along with the selected bond parameters and an atom-labeling scheme. The isolated one-water complex in the S_0 state, *trans*-HCOOH−$H_2O(S_0)$, has a six-membered ring structure and the two intermolecular hydrogen bonds are almost coplanar with one of the O−H bonds of water outside the ring plane. The H5···O6 and H7···O3 distances are, respectively, 1.942 and 2.369 Å in the *trans*-HCOOH−$H_2O(S_0)$ complex. The C1−O4 bond length is decreased by 0.012 Å in the complex in comparison with that in the free HCOOH molecule. The intramolecular O−H bonds in the H-bonded ring are slightly increased by formation of complex. With the effects from the bulk surrounding H_2O molecules considered, the H5···O6 distance becomes 1.820 Å, which is very close to the value of 1.810 Å inferred experimentally.[48] As shown in Figure 1, the cyclic H-bond structure of *trans*-HCOOH−$H_2O(S_0)$ is opened by the effects of bulk H_2O environment with a H7···O3 distance of 3.589 Å.

Upon electronic excitation to the S_1 state the most striking changes in structure are associated with the C1−O3 and C1−O4 bond lengths, which are, respectively, 1.219 and 1.318 Å in *trans*-HCOOH−$H_2O(S_0)$ and become 1.398 and 1.371 Å in the S_1 state of *trans*-HCOOH−$H_2O(S_1)$. It is easy to understand that the $n \rightarrow \pi^*$ electronic transition reduces the π-bonding character of the carbonyl group and destroys the conjugation interaction between the π electrons and the lone electron pair of the O4 atom. In addition, the two O4−H5···O6 and O6−H7···O3 H-bond structures, which are almost coplanar in the S_0 state, are not coplanar in the S_1 state due to rehybridization of the C atom from sp^2 to sp^3. The H5···O6 and H7···O3 distances are, respectively, 1.968 and 2.956 Å in the *trans*-HCOOH−$H_2O(S_1)$ structure, which are 0.026 and 0.587 Å

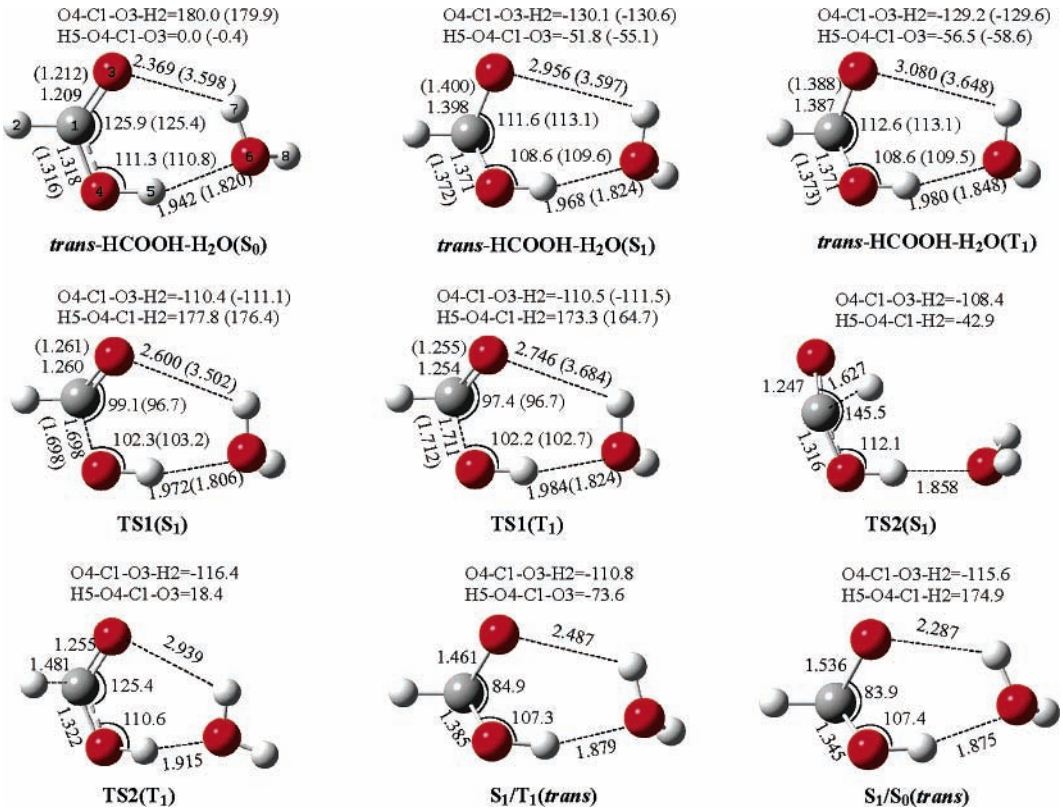

Figure 1. Schematic structures of the stationary and intersection points for the HCOOH−H_2O complex in the S_0, T_1, and S_1 states along with the selected CAS(10,8)/cc-pVTZ bond parameters.

longer than the corresponding values in the S_0 structure. It is obvious that the intermolecular hydrogen bonds are significantly weakened after the complex is excited to the S_1 state.

Like the complex in the S_1 state, the intermolecular H-bond interaction is much weaker in the T_1 complex [*trans*-HCOOH−$H_2O(T_1)$] than that in *trans*-HCOOH−$H_2O(S_0)$. The intermolecular H5···O6 and H7···O3 distances are, respectively, 1.980 and 3.080 Å in *trans*-HCOOH−$H_2O(T_1)$ and 0.038 and 0.711 Å longer than the corresponding values in *trans*-HCOOH−$H_2O(S_0)$. From a general understanding of hydrogen-bond formation,[50] the lone electron pair of the O3 atom plays a key role in formation of the O6−H7···O3 hydrogen bond. In the S_0 state the O6−H7···O3 hydrogen-bonding interaction is relatively strong because of the lone electron pair donor at the O3 atom. However, after HCOOH is excited to the S_1 or T_1 state, one nonbonding electron is excited from the oxygen atom to the antibonding π^* orbital in the carbonyl group, and this leads to a decrease of the electron density on the O3 atom. As a consequence, the O6−H7···O3 hydrogen bond is severely weakened in the S_1 or T_1 state in comparison with that in the ground state.

The bulk surrounding H_2O molecules have a noticeable influence on the structures of *trans*-HCOOH−$H_2O(T_1)$ and *trans*-HCOOH−$H_2O(S_1)$. The H5···O6 bond distance is decreased from 1.968 Å in gaseous *trans*-HCOOH−$H_2O(S_1)$ complex to 1.824 Å in aqueous *trans*-HCOOH−$H_2O(S_1)$ complex. However, the H7···O3 distance becomes 3.597 Å for the *trans*-HCOOH−$H_2O(S_1)$ complex in the aqueous phase. A similar situation was found for the complex in the S_0 state. The relatively strong H bond in the HCOOH−H_2O complex becomes stronger and the relatively weak H bond is completely broken on going from the gas phase to solution. The opened HCOOH−H_2O complex has a bigger dipole moment than the cyclic complex. As a result, the solvation energy of the opened complex is larger than the cyclic complex. This is the main reason that the opened complex becomes more stable in the aqueous phase. In the neutral complexes of acetic acid with acetaldehyde, acetamide, ammonia, methanol, and phenol[51] the weaker of the two hydrogen bonds in the complex was observed to be opened and the strong hydrogen bond was found to be shortened with increasing polarity of the solvent from heptane to DMSO to water.

Experimentally, the band origin has been identified as 37413.4 cm^{-1} (107.0 kcal·mol^{-1}) in the $S_0 \rightarrow S_1$ spectrum of gas-phase formic acid.[52] In aqueous solution, the absorption maximum was located at 207 nm by femtosecond transient absorption spectroscopy, which is blue shifted by ~8 nm (~0.2 eV) relative to the peak position of the gas-phase spectrum.[37] The $n \rightarrow \pi^*$ vertical transition in HCOOH−$(H_2O)_n$ ($n = 1-5$) complexes have been studied using the CAS(2,2) and subsequent second-order perturbation theory (CASPT2), and the absorption maximum was predicted to be blue shifted by 0.2−0.4 eV.[53,54] The MR−CI single-point calculations on the CAS(10,8)-optimized structures for the HCOOH−H_2O complex give a $S_0 \rightarrow S_1$ adiabatic excitation energy of 110.2 kcal·mol^{-1}. In comparison to the MR-CI result of 107.7 kcal·mol^{-1} for free HCOOH molecule,[32] the adiabatic excitation energy is increased by 2.5 kcal·mol^{-1} upon complex formation. With respect to the S_0 zero level, the T_1 state has its relative energy of 105.8 kcal·mol^{-1} for the free HCOOH molecule and 108.0 kcal·mol^{-1} for the one-water complex of formic acid. These results are consistent with the experimental fact that the absorption peak is blue shifted.

The solvent effect from bulk water molecules was included to predict the $S_0 \rightarrow S_1$ adiabatic excitation energy by applying the PCM model at the CAS(10,8) level. The adiabatic excitation energy is increased by ~0.5 kcal·mol^{-1} for the complex in the bulk water environment. It is evident that the bulk water

molecules have little influence on the excitation energy of formic acid in aqueous solution. The reason for this comes from a narrow change of dipole moments from *trans*-HCOOH−$H_2O(S_0)$ to *trans*-HCOOH−$H_2O(S_1)$. The blue-shifted transition observed in the absorption spectrum of aqueous HCOOH is attributed to the hydrogen-bonding effect from the explicit water in the complex. Charge transfer from the O to C atom occurs in the C═O group upon n → π^* excitation, and the interaction between HCOOH and H_2O is weakened when the complex is excited from S_0 to S_1. As a result, the intermolecular H bonds in *trans*-HCOOH−$H_2O(S_1)$ are weaker than those in *trans*-HCOOH−$H_2O(S_0)$ and the HCOOH−H_2O complex in the S_1 state has a relatively higher energy than the isolated HCCOH molecule in the S_1 state.

B. C−O Single-Bond Fission. The free HCOOH molecules in the S_0, S_1, and T_1 states can correlate with the fragments of OH($\tilde{X}^2\Pi$) + HCO($\tilde{X}^2A'$) in the ground state. The state correlation diagram for dissociation processes of the free HCOOH molecule will not be changed by formation of complex with water. No barrier was found above the endothermic character on the S_0 pathway from *trans*-HCOOH−$H_2O(S_0)$ to OH($\tilde{X}^2\Pi$)−H_2O + HCO($\tilde{X}^2A'$). The dissociation process is endothermic by 95.7 kcal·mol^{-1} at the CAS(10,8) level, which is 7.3 kcal·mol^{-1} lower than that for the free HCOOH molecule.

On the S_1 pathway, however, both experimental[20,21] and theoretical investigations[32] on the gas-phase photodissociation of *trans*-HCOOH showed that a barrier exists on the C−O bond cleavage pathway. A transition state, labeled as TS1−$H_2O(S_1)$, was found for *trans*-HCOOH−$H_2O(S_1)$ dissociation to OH($\tilde{X}^2\Pi$)-H_2O + HCO($\tilde{X}^2A'$) and confirmed to be the first-order saddle point by frequency calculations. As shown in Figure 1, the C1−O4 bond is nearly broken in the TS1−$H_2O(S_1)$ structure and the C1−O3 bond is significantly shortened from *trans*-HCOOH−$H_2O(S_1)$ to TS1−$H_2O(S_1)$. In addition, in the TS1−$H_2O(S_1)$ structure the H7···O3 distance decreases from 2.965 to 2.600 Å due to an increase of electron density on the O3 atom. The barrier height for *trans*-HCOOH−$H_2O(S_1)$ dissociation to OH($\tilde{X}^2\Pi$)−H_2O + HCO($\tilde{X}^2A'$) was estimated to be 14.4 and 14.8 kcal·mol^{-1} by the CAS(10,8) and MR-CI calculations with the CAS(10,8) zero-point energy corrections, respectively, which is slightly higher than the value of 13.5 kcal·mol^{-1} for the gas-phase dissociation of *trans*-HCOOH.[32] The potential-energy profiles for the C−O bond cleavage are shown in Figure 2.

A similar transition state on the T_1 potential-energy surface, TS1−$H_2O(T_1)$, is obtained by the B3LYP and CAS(10,8) optimizations. The resulting structure is shown in Figure 1 along with the CAS(10,8) bond parameters. TS1−$H_2O(T_1)$ is similar to TS1−$H_2O(S_1)$ in structure. The barrier height on the T_1 pathway is 13.4 and 14.5 kcal·mol^{-1} at the B3LYP and CAS(10,8) levels, respectively, which is very close to that on the S_1 pathway. It was recognized on that the S_0 → S_1 electronic spectrum of HCOOH possesses a rich vibrational structure in the 268−250 nm[52] that becomes diffuse at ∼250 nm and eventually merged into a continuum at wavelengths shorter than 225 nm. This shows that the barrier to the S_1 dissociation is in the range of 7.5−20.0 kcal·mol^{-1}. The calculated barrier height is reasonable, as compared with the experimental findings. The CH_3COOH dissociation into CH_3CO + OH along the S_1 pathway was found to have a barrier of 13−15 kcal·mol^{-1} from previous experimental and theoretical studies,[55−58] which is very close to the present calculated value for the *trans*-HCOOH−$H_2O(S_1)$ dissociation to OH($\tilde{X}^2\Pi$)−H_2O + HCO($\tilde{X}^2A'$).

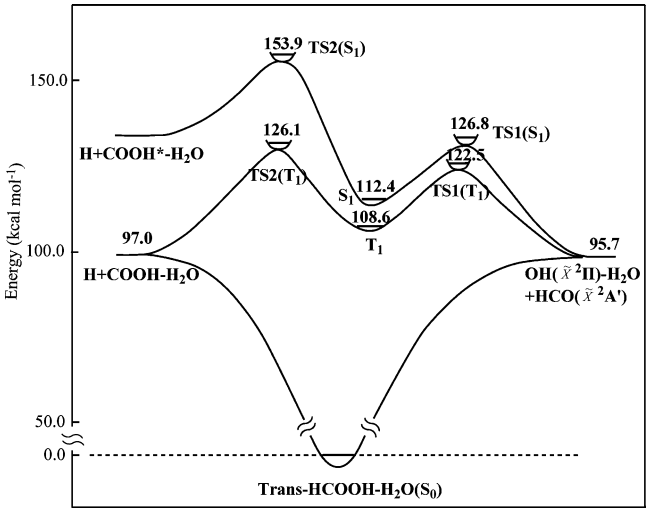

Figure 2. Schematic S_0, T_1, and S_1 potential-energy surfaces for the *trans*-HCOOH−H_2O dissociations to HO−H_2O + HCO and H + COOH−H_2O along with the CAS(10,8)/cc-pVTZ relative energies (kcal/mol).

C. Dissociation of the HCOOH−H_2O Complex into H + COOH−H_2O. Except for the C−O bond fission channel, the process for *trans*-HCOOH dissociation into H + COOH could contribute to the photolysis of formic acid molecules following excitation within their S_0 → S_1 absorption system. A qualitative analysis from the correlation rules indicates that the ground-state radicals of COOH ($^2A'$) + H(^2S) can correlate with S_0 and T_1 states of *trans*-HCOOH in C_1 symmetry. On the S_0 pathway it was a endothermic process for *trans*-HCOOH dissociation into COOH ($^2A'$) + H(^2S). The dissociation energy was estimated to be 93.3 kcal·mol^{-1} in previous work.[32] After taking the HCOOH−H_2O complex as the system in the present work, the HCOOH−H_2O dissociation into H + COOH−H_2O is determined to be endothermic by 97.0 kcal·mol^{-1} from a supermolecular calculation at the CAS(10,8) level.

The structure of the transition state for C−H bond cleavage on the T_1 surface was obtained by full optimization at the CAS-(10,8) level. Following optimization frequency calculation was carried out to confirm the optimized transition state to be a real first-order saddle point, referred to as TS2−$H_2O(T_1)$ in Figure 1 along with the selected bond parameters. Note that the H_5···O_6 distance is shortened by 0.069 Å in TS2−$H_2O(T_1)$, which suggests that a stronger hydrogen-bonding interaction between COOH moiety and H_2O comes into being. The dihedral angle of H5−O4−C1−O3 varies from −56.5° in T_1 to 18.4° in TS2−$H_2O(T_1)$, resulting in a nearly coplanar structure for the COOH fragment. The barrier height for the C−H bond fission on the T_1 pathway is predicated to be 18.1 kcal·mol^{-1} by the CAS(10,8) calculations. For comparison, the TS2−$H_2O(T_1)$ structure is re-optimized at the B3LYP level. The B3LYP- and CAS(10,8)-optimized bond parameters are close to each other, but the barrier height is reduced to 12.5 kcal·mol^{-1} by the B3LYP calculations. The potential-energy profiles for C−H bond cleavage are shown in Figure 2.

To explore the possibility that the HCOOH−H_2O complex dissociates into H + COOH−H_2O along the S_1 pathway, a transition state for C−H bond fission on the S_1 surface was optimized at the CAS(10,8) level. The optimized structure is given in Figure 1, labeled as TS2−$H_2O(S_1)$ hereafter, which was confirmed to be the first-order saddle point by frequency analysis. It should be noted that this transition state differs greatly from TS2−$H_2O(T_1)$ in structure. The C−H distance in TS2−$H_2O(S_1)$ is 0.164 Å longer than that in TS2−$H_2O(T_1)$.

SCHEME 1

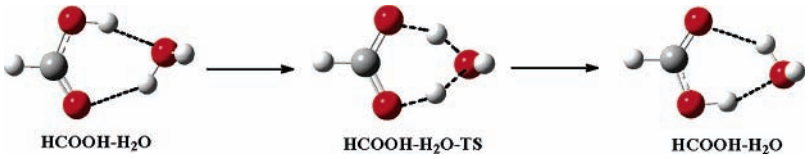

The most remarkable change is the O3−C1−O4 angle, which is increased from 125.4° in TS2−$H_2O(T_1)$ to 145.5° in TS2−$H_2O(S_1)$. Meanwhile, the H5···O6 distance is shortened to 1.858 Å in TS2−$H_2O(S_1)$ from 1.915 Å in TS2−$H_2O(T_1)$. The dihedral angles of H5−O4−C1−H2 and H5−O4−C1−O3 are, respectively, −42.9° and 65.5° in TS2−$H_2O(S_1)$, which are dramatically increased by 48.8° and 47.1° in comparison with those in TS2−H_2O (T_1). The barrier height was predicted to be 41.5 and 36.5 kcal·mol^{-1} at the CAS(10,8) and MR-CI levels, respectively, with the CAS(10,8) zero-point energy correction. This barrier is much higher than that on the T_1 pathway. S_1 dissociation leads to fragments in the excited state, while T_1 dissociation results in the fragments in the ground state. This is the main reason that the relatively high barrier exists on the S_1 pathway and there is large difference in the TS2−$H_2O(T_1)$ and TS2−$H_2O(S_1)$ structures.

Here we pay little attention to other possible reaction processes. O−H bond cleavage was observed in the VUV dissociation[20] of HCOOH at an excitation energy of 12 eV, which shows that O−H bond cleavage occurs very difficultly for HCOOH in the gas phase. The O−H bond of HCOOH is weakened upon formation of the cyclic HCOOH−H_2O complex. It could be expected that the O−H bond cleavage of HCOOH proceeds more easily in the complex than in the isolated HCOOH molecule. All attempts to optimize a transition state for the O−H bond fission in the S_0 state lead to a structure that is confirmed to be the transition state connecting the two equivalent *trans*-HCOOH−$H_2O(S_0)$ complexes. An analogous situation was found for the S_1 state. Actually, the O−H bond fission for HCOOH in the gas phase is changed into a tautomerization reaction in aqueous formic acid, as shown in Scheme 1. Examination of the *trans*-HCOOH−$H_2O(S_0)$ structure in Figure 1 shows that molecular elimination to CO + H_2O takes place more easily in the complex than in the isolated HCOOH molecule. However, isomerization from *trans*-HCOOH−$H_2O(S_0)$ to *cis*-HCOOH−$H_2O(S_0)$ takes place prior to molecular elimination to CO_2 + H_2. Since a relatively strong hydrogen bond is formed in the *trans*-HCOOH−$H_2O(S_0)$ complex, molecular elimination to CO_2 + H_2 occurs more difficultly in the complex, as compared with that in the isolated HCOOH molecule. Thus, molecular elimination to CO + H_2O is the dominant pathway once the complex is in the ground state.

Before the end of this subsection we discuss the hydrogen-bonding effect from two or more water molecules in the complex. Many minimum-energy structures have been found for complexes of formic acid with one, two, and three water molecules in the ground state.[46−48] However, the most stable conformation has a cyclic structure for each complex. The transition states of proton transfer in the cyclic two- and three-water complexes were confirmed to connect the two equivalent minima, and the barrier heights were predicted to be about 16 kcal·mol^{-1} by DFT and MP2 calculations,[59] which is similar to that for the cyclic one-water complex (Scheme 1). The cyclic structures for the two-water complexes in the S_0 and S_1 states and the transition state of the S_1 C−O single bond cleavage were optimized at the CAS(10,8) level in the present work. The $S_0 \rightarrow S_1$ adiabatic excitation energy was found to decrease slightly, but the barrier energy of the S_1 C−O single-bond cleavage is nearly unchanged from the one-water to two-water complex. It is reasonable to expect that possible dissociation channels for complexes of the formic acid with two or more water molecules are the same as those for the one-water complex.

D. Surface Intersection and Mechanistic Aspects. Structural optimization of the S_1 and S_0 surface intersection for the one-water complex was carried out by searching for the lowest energy point of the surface crossing seam at the state-averaged CAS(10,8) level. The resulting structure, referred to as S_1/S_0, is shown in Figure 1. The C1−O3 and C1−O4 distances are, respectively, 1.536 and 1.345 Å in the S_1/S_0 structure, which differ from the corresponding values of 1.398 and 1.371 Å in the S_1 equilibrium geometry. There are also some differences in bond angles and dihedral angles between the S_1/S_0 and S_1 structures, as can be seen from Figure 1. With respect to the S_1 minimum, the S_1/S_0 structure has its relative energy of 31.7 kcal·mol^{-1} at the CAS(10,8) level for the one-water complex, which is nearly the same as the relative energy (31.5 kcal·mol^{-1}) of the S_1/S_0 intersection for the HCOOH monomer.[32] The S_1 and T_1 surface intersection for the one-water complex (S_1/T_1) was optimized using Slater determinants in the state-averaged CAS(10,8) calculations. The obtained structure for the S_1/T_1 intersection is shown in Figure 1. In comparison with the S_1 equilibrium structure, the C1−O3 bond length is increased by 0.061 Å and the O3−C1−O4 angle is decreased by about 20° in the S_1/T_1 structure. Relative to the S_1 minimum, the S_1/T_1 structure has its relative energy of 21.1 kcal·mol^{-1} at the CAS-(10,8) level for the one-water complex. The relative energy of the S_1/T_1 intersection for the isolated HCOOH molecule is 24.6 kcal·mol^{-1} at the same level.[32]

Upon photoexcitation of aqueous HCOOH at ∼250 nm, which corresponds to an excitation energy of 112 kcal·mol^{-1}, the S_1 direct dissociations, intersystem crossing (ISC) via the T_1/S_1 point, and internal conversion (IC) through the S_0/S_1 point are all inaccessible in energy. In this case, the system relaxes mainly to the ground state via the S_0 and S_1 vibronic interaction besides radiation processes. After relaxation to the S_0 state, the system is left with sufficient internal energy to overcome the barriers on the S_0 pathways, leading to formation of CO + H_2O. Dissociation channels 1, 2, and 3 are highly endothermic along the S_0 pathways and are not in competition with molecular elimination in the ground state, leading to formation of CO + H_2O. Carbon monoxide was observed with considerable yield upon photolysis of aqueous formic acid at 253.7 nm.[35] Two separation pathways, HCOOH → HCO → CO and HCOOH → COOH → CO, were suggested to be responsible for formation of CO. The present calculation predicts that internal conversion to the S_0 state followed by molecular elimination is a possible pathway for formation of carbon monoxide. It should be pointed out that the quantum yield of internal conversion to the S_0 state is decreased by the interaction between the *trans*-HCOOH−$H_2O(S_1)$ complexes and H_2O molecules in the aqueous environment. As a result, molecular elimination to CO + H_2O is a minor channel upon photolysis of aqueous formic acid.

The HCOOH−H_2O complexes populated in S_1 by photoexcitation at ∼200 nm possess internal energies of ∼140 kcal·mol^{-1}. Under this condition, S_1 direct dissociation to OH($\tilde{X}^2\Pi$)−H_2O + HCO($\tilde{X}^2A'$) and intersystem crossing via the T_1/S_1 point are favorable in energy. The initial photoexcitation is localized on the C═O region, and the relatively large forces (energy gradients) are at the directions of the C═O stretching and O−C−O bending motions, which control the redistribution of the initial excitation energies in the stretching and bending modes. As can be seen from Figure 1, relaxation from the S_1 Franck−Condon geometry to the T_1/S_1 intersection involves mainly the C═O stretching and O−C−O bending vibrations. The relaxation process is expected to take place within a few vibrational periods. The C1−O3 bond distance is 1.461 Å in the S_1/T_1 structure for the one-water complex, while this distance is 1.641 Å in the S_1/T_1 structure for the isolated HCOOH molecule.[32] The relative energy of the S_1/T_1 structure is reduced by 3.5 kcal·mol^{-1} from the isolated HCOOH molecule to its complex with one water. It is evident that the $S_1 \rightarrow T_1$ intersystem crossing becomes more efficient in the aqueous environment.

As discussed above, the barrier height of the C−O bond fission for the one-water complex on the S_1 pathway is nearly equal to that for the isolated HCOOH molecule. The rate of C−O bond cleavage is less influenced by formation of complex and the bulk water molecules. The rate constant is estimated to be on the order of 10^9 s^{-1} with the excitation energy at 140 kcal·mol^{-1}. Femtosecond transient absorption spectroscopy was used to investigate the primary reaction dynamics of aqueous formic acid following photoexcitation at 200 nm.[37] It was found that aqueous formic acid dissociates predominantly into fragments of HCO and OH, which is consistent with the calculated result. The measured transient absorption shows that a dark channel exists with a time constant of ∼170 ps.[37] This dark channel is assigned as fast relaxation from the S_1 Franck−Condon geometry to the T_1/S_1 intersection and subsequent $S_1 \rightarrow T_1$ intersystem crossing process at the intersection.

Summary

Photodissociation of aqueous formic acid has been investigated with CASSCF, DFT, and MR-CI methods. Solvent effects are considered as a combination of the hydrogen-bonding interaction from explicit H_2O molecules and the effects from the bulk surrounding H_2O molecules using the polarizable continuum model. It is found that the intermolecular hydrogen bonds between HCOOH and H_2O are significantly weakened after the HCOOH−H_2O complex is excited to the S_1 state, which is mainly responsible for the blue-shifted transition observed in the absorption spectrum of aqueous formic acid. The cyclic H-bond structures for the one-water complexes in the ground and excited states are opened by the effects of the bulk H_2O environment. The quantum yield of the $S_1 \rightarrow S_0$ internal conversion is decreased by the interaction between the excited complexes and H_2O molecules in the aqueous environment. However, the $S_1 \rightarrow T_1$ intersystem crossing becomes more efficient in the aqueous environment due to geometric effects that control the initial relaxation dynamics after photoexcitation. The hydrogen-bonding effect from the explicit water in the complex is the major factor to influence physical properties of aqueous formic acid, while the bulk surrounding H_2O molecules have a noticeable influence on the structures of the complexes in the ground and excited states.

The barrier height of the C−O bond fission for the one-water complex on the S_1 pathway is nearly equal to that for the isolated HCOOH molecule. The rate constant of the C−O bond cleavage is less influenced by formation of the complex and bulk water molecules. Because of a barrier of about 14.5 kcal·mol^{-1} on the S_1 pathway, the direct C−O bond fission along the S_1 pathway becomes an important channel upon photolysis of aqueous formic acid at 200 nm. Femtosecond transient absorption spectroscopy study shows that aqueous formic acid dissociates predominantly into fragments of HCO and OH, which is supported by the present calculation. The measured transient absorption shows that a dark channel exists upon photolysis of aqueous formic acid at 200 nm, which is assigned as fast relaxation from the S_1 Franck−Condon geometry to the T_1/S_1 intersection and a subsequent $S_1 \rightarrow T_1$ intersystem crossing process. Molecular elimination to CO + H_2O in the ground state takes place more easily in the complex than in the isolated HCOOH molecule. However, molecular elimination to CO_2 + H_2 occurs more difficultly in the complex as compared with that in the isolated HCOOH molecule. $S_1 \rightarrow S_0$ internal conversion followed by molecular elimination to CO + H_2O is the most probable primary process for formation of carbon monoxide, which was observed with considerable yield upon photolysis of aqueous formic acid at 253.7 nm. O−H bond fission for HCOOH in the gas phase is changed into a tautomerization reaction in aqueous formic acid. C−H bond fission was not observed experimentally due to a high barrier on the fission pathway.

Acknowledgment. This work was supported by grants from the National Natural Science Foundation of China (grant nos. 20472011, 20233020, and 20573011) and Major State Basic Research Development Programs (grant nos. 2004CB719903 and 2002CB613406).

Supporting Information Available: Structures and energies for all stationary points reported in the present work. This material is available free of charge via the Internet at http://pubs.acs.org.

References and Notes

(1) Gardiner, W. C., Jr. *Combustion Chemistry*; Springer-Verlag: Berlin, 1984; p 294.
(2) Kaiser, R. I. *Chem. Rev.* **2002**, *102*, 1309−1358.
(3) Khwaja, H. A. *Atmos. Environ.* **1995**, *29*, 127−139.
(4) Chapman, E. G.; Kenny, D. V.; Busness, K. M.; Thorp, J. M.; Spicer, C. W. *Geophys. Res. Lett.* **1995**, *22*, 405−408.
(5) Ramsperger, H. C.; Porter, C. W. *J. Am. Chem. Soc.* **1926**, *48*, 1267.
(6) Gorin, E.; Taylor, H. S. *J. Am. Chem. Soc.* **1934**, *56*, 2042.
(7) Burton, M. *J. Am. Chem. Soc.* **1936**, *58*, 1655.
(8) Gorden, R., Jr.; Ausloos, P. *J. Phys. Chem.* **1961**, *65*, 1033.
(9) Jolly, G. S.; McKenney, D. J.; Singleton, D. L.; Paraskevopoulos, G.; Bosard, A. R. *J. Phys. Chem.* **1986**, *90*, 6557.
(10) Singleton, D. L.; Paraskevopoulos, G.; Irwin, R. S.; Jolly, G. S.; McKenney, D. J. *J. Am. Chem. Soc.* **1988**, *110*, 7786.
(11) Singleton, D. L.; Paraskevopoulos, G.; Irwin, R. S. *J. Am. Chem. Soc.* **1989**, *111*, 5248.
(12) Jolly, G. S.; Singleton, D. L.; McKenney, D. J.; Paraskevopoulos, G. *J. Chem. Phys.* **1986**, *84*, 6662.
(13) Jolly, G. S.; Singleton, D. L.; Paraskevopoulos, G. *J. Phys. Chem.* **1987**, *91*, 3463.
(14) Singleton, D. L.; Paraskevopoulos, G.; Irwin, R. S. *J. Phys. Chem.* **1990**, *94*, 695−699.
(15) Irwin, R. S.; Singleton, D. L.; Paraskevopoulos, G.; Mclaren, R. *Int. J. Chem. Kinet.* **1994**, *26*, 219.
(16) Ebata, T.; Amano, T.; Ito, M. *J. Chem. Phys.* **1989**, *90*, 112.
(17) Brouard, M.; Omahony, J. *Chem. Phys. Lett.* **1988**, *149*, 45. Brouard, M.; Simons, J. P.; Wang, J. X. *Faraday Discuss. Chem. Soc.* **1991**, *91*, 63−72.
(18) Su, H.; He, Y.; Kong, F.; Fang, W.-H.; Liu, R.-Z. *J. Chem. Phys.* **2000**, *113*, 1891−1897.
(19) Khriachtchev, L.; Macoas, E.; Rasanen, M. *J. Am. Chem. Soc.* **2002**, *124*, 10994−10995.

(20) Schwell, M.; Dulieu, F.; Jochims, H.-W.; Fillion, J.-H.; Lemaire, J.-L.; Baumgartel, H.; Leach, S. *J. Phys. Chem. A* **2002**, *106*, 10908−10918.
(21) Peterson, M. R.; Csizmadia, I. G. *J. Am. Chem. Soc*. **1979**, *101*, 1076.
(22) Wiberg, K. B.; Laidig, K. E. *J. Am. Chem. Soc*. **1987**, *109*, 5935.
(23) Chang, Y.-T.; Yamaguchi, Y.; Miller, W. H.; Schaefer, H. F., III *J. Am. Chem. Soc*. **1987**, *109*, 7245.
(24) Fausto, R.; Batistade de Carvallo, L. A. E.; Teixeria-Dias, J. J. C.; Ramos, M. N. *J. Chem. Soc., Faraday Trans II* **1989**, *85*, 1945.
(25) Feller, D.; Bordon, W. T.; Davidson, E. R. *J. Comput. Chem.* **1980**, *1*, 158.
(26) Feller, D.; Bordon, W. T.; Davidson, E. R. *J. Chem. Phys*. **1979**, *71*, 4987.
(27) Ruelle, P.; Kesselring, U. W.; Nam-Tran, H. *J. Am. Chem. Soc*. **1986**, *108*, 371−375.
(28) Ruelle, P. *J. Am. Chem. Soc*. **1987**, *109*, 1722.
(29) Francisco, J. S. *J. Chem. Phys*. **1992**, *96*, 1167.
(30) Goddard, J. D.; Yamaguchi, Y.; Schaefer, H. F., III *J. Chem. Phys*. **1992**, *96*, 1158−1168.
(31) Lundell, J.; Rasanen, M. *J. Mol. Struct.* **1997**, *436/437*, 349−358.
(32) He, H.-Y.; Fang, W.-H. *J. Am. Chem. Soc.* **2003**, *125*, 16139−16147.
(33) Martínez-Nunez, E.; Vazquez, S.; Granucci, G.; Persico, M.; Estevez, C. M. *Chem. Phys. Lett.* **2005**, *412*, 35−40.
(34) Kurosaki, Y.; Yokoyama, K.; Teranishi, Y. *Chem. Phys.* **2005**, *308*, 325−334.
(35) Adams, G. E.; Hart, E. J. *J. Am. Chem. Soc*. **1962**, *84*, 3994−3999.
(36) Karpel, N.; Leitner, V.; Dore, M. *New J. Chem.* **1995**, *19*, 1171−1176.
(37) Thøgersen, J.; Jensen, S. K.; Christiansen, O.; Keiding, S. R. *J. Phys. Chem. A* **2004**, *108*, 7483−7489.
(38) Lee, K. W.; Lee, K.-S.; Jung, K.-H.; Volpp, H.-R. *J. Chem. Phys*. **2002**, *117*, 9266−9274.
(39) Pettersson, M.; Macoas, E. M. S.; Khriachtchev, L.; Lundell, J.; Fausto, R.; Rasanen, M. *J. Chem. Phys.* **2002**, *117*, 9095−9098.
(40) Schmidt, M. W.; Gordon, M. S. *Annu. Rev. Phys. Chem.* **1998**, *49*, 233−266.
(41) Dunning, T. H., Jr. *J. Chem. Phys*. **1989**, *90*, 1007. Woon, D. E.; Dunning, T. H., Jr. *J. Chem. Phys.* **1993**, *98*, 1358. Peterson, K. A.; Woon, D. E.; Dunning, T. H., Jr. *J. Chem. Phys*. **1994**, *100*, 7410.
(42) Cossi, M.; Barone, V.; Robb, M. A. *J. Chem. Phys.* **1999**, *111*, 5295.
(43) Barone, V.; Cossi, M.; Tomasi, J. *J. Chem. Phys.* **1997**, *107*, 3210.
(44) Frisch, M. J. et al. *Gaussian 03*, Revision B.02; Gaussian, Inc.: Pittsburgh, PA, 2003.
(45) MOLPRO is a package of ab initio programs written by Werner, H.-J. and Knowles, P. J. with contributions from Amos, R. D. et al.
(46) Aloisio, S.; Paul, E. H.; Veronica, V. *J. Phys. Chem. A* **2002**, *106*, 363−370.
(47) Zhou, Z.-Y.; Shi, Y.; Zhou, X.-M. *J. Phys. Chem. A* **2004**, *108*, 813−822.
(48) Priem, D.; Ha, T. K.; Bauder, A. *J. Chem. Phys.* **2000**, *113*, 169−175.
(49) Astrand, P. O.; Karlström, G.; Engdahl, A.; Nelander, B. *J. Chem. Phys.* **1995**, *102*, 3534−3554.
(50) Kollman, P. A.; Allen, L. C. *Chem. Rev*. **1972**, *72*, 283−303.
(51) Aquino, A. J. A.; Tunega, D.; Haberhauer, G.; Gerzabek, M. H.; Lischka, H. *J. Phys. Chem. A* **2002**, *106*, 1862−1871.
(52) Beaty-Travis, L. M.; Moule, D. C.; Liu, H.; Lim, E. C.; Judge, R. H. *J. Mol. Spectrosc.* **2001**, *205*, 232−238. Beaty-Travis, L. M.; Moule, D. C.; Lim, E. C.; Judge, R. H. *J. Chem. Phys*. **2002**, *117*, 4831−4838.
(53) Velardez, G.; Heully, J. L.; Beswick, J. A.; Daudey, J. P. *Phys. Chem. Commun.* **1999**, 6.
(54) Velardez, G.; Ferrero, J. C.; Beswick, J. A.; Daudey, J. P. *J. Phys. Chem. A* **2001**, *105*, 8769−8774.
(55) Hunnicutt, S. S.; Waits, L. D.; Guest, J. A. *J. Phys. Chem.* **1989**, *93*, 5188.
(56) Hunnicutt, S. S.; Waits, L. D.; Guest, J. A. *J. Phys. Chem.* **1991**, *95*, 562.
(57) Peterman, D. R.; Daniel, R. G.; Horwitz, R. J.; Guest, J. A. *Chem. Phys. Lett.* **1995**, *236*, 564.
(58) Fang, W. H.; Liu, R. Z.; Zheng, X.; Phillips, D. L. *J. Org. Chem*. **2002**, *67*, 8407−8415.
(59) Wei, D. Q.; Truchon, J.-F.; Sirois, S.; Salahub, D. *J. Chem. Phys.* **2002**, *116*, 6028−6038.